Biotechnol. Bioprocess Eng. **2001**, 6: 376-385

Recent Trends in the Biosorption of Heavy Metals: A Review

Yeşim Sağ* and Tülin Kutsal

Hacettepe University, Faculty of Engineering, Department of Chemical Engineering, 06532, Beytepe, Ankara, Turkey

Abstract Considerable attention has been focused in recent years upon the field of biosorption for the removal of metal ions from aqueous effluents. Compared to other technologies, the advantages of biosorption are the high purity of the treated waste water and the cheap raw material. Really, the first major challenge for the biosorption field is to select the most promising types of biomass. Abundant biomass types either generated as a waste by-product of large-scale industrial fermentations particularly fungi or certain metal-binding seaweeds have gained importance in recent years due to their natural occurrence, low cost, and, of course, good performance in metal biosorption. Industrial solutions commonly contain multimetal systems or several organic and inorganic substances that form complexes with metals at relatively high stability forming a very complex environment. When several components are present, interference and competition phenomena for sorption sites occur and lead to a more complex mathematical formulation of the process. The most optimal configuration for continuous flow-biosorption seems to the packed-bed column which gets gradually saturated from the feed to the solution exit end. Owing to the competitive ion exchange taking place in the column, one or more of the metals present even at trace levels may overshoot the acceptable limit in the column effluent before the breakthrough point of the targeted metal. Occurrence of 'overshoot's and impact on heavy metal removal has not been analyzed enough. New trends in biosorption are discussed in this review.

Keywords: waste water, heavy metal ions, biosorption, mathematical modelling

INTRODUCTION

The search for new technologies involving the removal of toxic metals from waste waters has directed attention to biosorption, based on the metal binding capacities of various biological material. Developments in the field of environmental biotechnology indicate that bacteria, actinomycetes, fungi, yeasts, algae and seaweeds can remove heavy metals from aqueous solutions by biosorption. Although the complexity of the microorganism's structure implies that there are many ways for the metal to be captured by the cell, biosorption mechanisms can be divided mainly into: (i) metabolism dependent and (ii) non-metabolism dependent [1]. In the case of physicochemical interaction between the metal and functional groups of the cell surface, based on physical adsorption [2], ion exchange [3] and complexation [4], there is cell surface sorption, which is not dependent on the metabolism. Cell walls of microbial biomass, mainly composed of polysaccharides, proteins and lipids, offer plentiful sorption, ion exchange, and covalent binding sites including carboxyl, hydroxyl, sulfhydryl, amino, and phosphate groups [5]. In the case of precipitation, the classification is not unique. The precipitation of the metal may take place both in solution and on the cell surface. It may be dependent on the cells' metabolism, *e.g.*, in the presence of toxic metals, the microorganism produces compounds which favour the precipitation process. In the case of precipitation not dependent on the cellular metabolism, it may be a consequence of the chemical interaction between the metal and the cell surface [1,6]. Transport across cell membrane, intracellular accumulation, is associated with cell metabolism [7]. Algae, fungi and bacteria differ from each other in their constitution, giving rise to different mechanisms of metal biosorption. To explore the biosorption mechanisms, it is necessary to identify the functional groups involved in the biosorption process.

* **Corresponding author**
Tel: +90-312-2977444 Fax: +90-312-2992124
e-mail: yesims@hacettepe.edu.tr

COMPARISON OF VARIOUS BIOMASS TYPES

Bacteria have polysaccharide slime layers and readily provide amino, carboxyl, phophate and sulphate groups for metals biosorption [8]. Bacterial biomass is generally produced as a waste by-product of industrial operations or can be specifically propagated in large scale. The uptake capacities of bacteria generally range between 0.23 to 0.90 mmol/g [9,10].

Some types of industrial fermentation waste biomass are really excellent metal sorbers. For that reason, fungi, including yeasts, have received increased attention.

Fungi can also be grown using unsophisticated fermentation techniques and inexpensive growth media or even waste carbohydrate-containing growth media based on *e.g.*, molasses or cheese whey. The eukaryotic microorganisms are always of unicellular nature; however, the vegetative phases of fungi and algae are frequently multicellular [11,12]. The sequestering of metallic species by fungal biomass has mainly been traced to the cell wall. Various polysaccharides are the main (up to 90%) constituents of the fungal cell wall. They are often complexed with proteins, lipids, and other substances (*e.g.*, pigments). Large quantities of phosphate and glucouronic acid and chitin-chitosan complex existing in these cell walls offer extensive possibilities for binding metals through ion exchange and coordination. In the fungal cell wall, several types of ionizable sites affect the metal uptake capacity: phosphate groups, carboxyl groups on uranic acids and proteins, and nitrogen-containing ligands on protein as well as on chitin or chitosan [5,13]. The surface of yeast cells can act as an ion exchange resin. Some 'waste' biomass is actually a commodity, not a waste, *e.g.*, brewer's yeasts and baker's yeasts sold on the open market for a price. The best-known yeast *Saccharomyces cerevisiae* possesses a mannan-glucan cell wall which contains only 1% chitin [13]. A wide range of biosorption capacities from 0.012 to 1.979 mmol/g for fungi has been reported [14,15]. A detailed comparison of heavy metal biosorption capacities of various free and immobilized fungi in different reactor systems has been just published in a comprehensive literature review on fungal biosorption [16]. White-rot fungi are a highly specialized group of organisms. They are *Basidiomycetes* which include all the higher fungi that are characterized by their sexual fruiting bodies. *Phanerochaete chrysosporium*, a well-known white-rot fungus, has been used for the biosorption of inorganic mercury ($HgCl_2$), methyl mercury (CH_3HgCl) and ethyl mercury (C_2H_5HgCl) [17]. A group of wood-rotting macro-fungi (*Ganoderma lucidum*, *Phellinus badius*) showed relatively higher capacities compared to micro-fungal biomass [18,19]. They can also be used in packed–bed columns without immobilization or chemical modification to enhance the structural strength of such biomass types. Some types of seaweed biomass offer excellent metal-sorbing properties while activated sludge from waste water treatment plants has not demonstrated high enough metal-sorbing capacities [20]. The metal uptake capacities exhibited by non-living biomass of micro-algal (green algae or fresh water algae) and macro-algal species (brown algae or marine algae) change from 0.066 to 1.20 mmol/g and 0.65 to 1.21 mmol/g, respectively [21-24].

Microalgae can sequester heavy metal ions by the same biosorption mechanisms as other microbial biomass as well as by the formation of phytochelatins which they synthesize in response to toxic heavy metal stress. Microalgae use light as an energy source, facilitating the maintanence of metabolism in the absence of organic carbon sources and electron acceptor required by bacteria or fungi. Thus, the use of metabolically active microalgal systems may be more readily achieved. Also, microalgae can be cultivated in open ponds or in large-scale laboratory culture, providing a reliable and consistent supply of biomass for eventual scale-up work. The two principal mechanisms involved in biosorption by microalgae appaer to be: (i) ion exchange wherein ions such as Na, Mg, and Ca become displaced by heavy metal ions, and (ii) complexation between metal ions and various functional groups such as carboxyl, amino, thiol, hydroxy, phophate, and hydroxy-carboxyl, that can interact in a coordinated way with heavy metal ions. Although thousands of micro-algal species have been identified, very few have been investigated for their biosorption potential, and the vast majority of studies have been conducted using unicellular green algae, principally *Chlorella vulgaris* and *Chlamydomonas reinhardtii* [25,26].

Some types of seaweed biomass offer excellent metal-sorbing properties, such as the brown seaweed *Sargassum fluitans*, *Durvillea potatorum* and *Ecklonia radiata*. The contribution of two potential ligands known to be present in the thallus of brown seaweeds, carboxyl and sulfonate groups, has been investigated at the molecular level qualitatively and quantitatively. Different strategies were employed in order to achieve this objective: potentiometric and conductometric titration, chemical analysis, modification of the biomass and infrared spectrophotometry [27-29].

DEPENDENCE OF THE BIOSORPTION PROCESS ON PH

Biosorbents can be viewed as natural ion-exchange materials that primarily contain weakly acidic and basic groups. The uptakes of heavy metal cations by most biomass types decrease dramatically as the pH of the metal solutions decreases from pH 6.0 to 2.5. The typical dependence of metal uptake on pH pointed to the weakly acidic carboxyl groups R-COOH (pK_a in the range 3.5-5.5) of algal and fungal cell-wall constituents as the probable sites of ion exchange [30]. Simultaneous potentiometric and conductimetric titrations of *Sargassum fluitans* gave some information concerning the amount of strong and weak acidic functional groups in the biomass (0.25 ± 0.05 and 2.00 ± 0.05 meq/g, respectively) [27]. The presence of strongly acidic sulfate groups ($R\text{-}OSO_3^-$) of fucoidan and carrageenan has been detected in the algae *Sargassum* and *Cladophora*, and these groups have been reported to represent 10% of the overall metal binding sites of these seaweeds. The contribution of amino groups of chitin ($R_2\text{-}NH$) and chitosan ($R\text{-}NH_2$) in fungi has also been examined. The ion exchange between protons and metals on amino groups is characterized by a pH dependence similar to that observed for carboxyl groups. However, the pH values at which the metal uptake increases sharply and reaches its maximum are generally higher for the amino groups than for the carboxyl groups [30].

NEW APPROACHES IN THE MODELLING OF BIOSORPTION OF HEAVY METALS

Adsorption isotherms are plots of the adsorbed sorbate quantity per unit weight of adsorbent, q_{eq}, at equilibrium and the final equilibrium concentration of the residual sorbate remaining in the solution, C_{eq}. The classical models of Langmuir, bi-Langmuir, Freundlich, and Redlich and Peterson are often used to describe the relationship. Equilibria and capacity relationships for monocomponent systems are well established and quantitatively expressed by various types of adsorption isotherms and are not reproduced here [4,31,32]. As also mentioned above, the metal ion binding mechanism in biosorption may involve different processes such as complexation, coordination, electrostatic attraction, or microprecipitation whereby ion exchange plays a major role in the binding of metal ions by algal biomass. Therefore, the use of ion exchange reaction constants instead of Freundlich- or Langmuir-type adsorption models has been suggested for describing the process. Since these unsophisticated isotherms do not account for the effect of the back reaction of the displaced ion and they cannot provide any mechanistic understanding of the biosorption phenomena, the latter is conveniently used to estimate the maximum uptake of metal from experimental data [33].

Fourest and Volesky showed that contribution of sulfate groups of the *Sargassum* biomass in metal binding is negligible as compared to carboxyl groups except for pH<3 where carboxyl groups become protonated [27]. Schiewer and Volesky derived a mathematical model for predicting the equilibrium of proton and metal ion binding as a function of metal ion concentration, pH, and ionic strength [34]. In the model derivation, it was assumed that only one type of binding site *C*, carboxyl group in the case of *Sargassum* is responsible for most of the metal binding. The binding of ions (protons=*H*, divalent metal ions=*M*) is defined as the sum of the coordinately (as $CX_{1/Zx}$) and electrostatically (as [*X*p]-[*X*]) bound ions:

$$^{H}q = CH + ([H_p]-[H])V_m \quad (1)$$

$$^{m}q = CM_{0.5} + 2([M_p]-[M])V_m \quad (2)$$

For any ionic species '*X*' with the charge Z_x, the concentrations [*X*] without subscript are the ones in the bulk solutions, $[X_p]$ is the average concentration of *X* in the particle, and V_m is the specific volume.

The reaction for the complexation of divalent metal ions *M* to a binding site *C* (*e.g.*, carboxyl for *Sargassum* seaweed biomass) is [34]

$$2C + M \Leftrightarrow 2CM_{0.5} \quad (3)$$

$$^{CM}K = \frac{CM_{0.5}^2}{C^2[M_p]} \quad (4)$$

The total number of binding sites stays constant during biosorption. For a two-metal ion system,

$$^{t}C = C + CH + CM1_{0.5} + CM2_{0.5} \quad (5)$$

The apparent *C* site proton binding constant is [35]

$$^{CH}K_{app} = \frac{CH}{C[H]} \quad (6)$$

The isotherm for the proton and metal ion binding can be derived from the binding constants for metal ions (Eq. (4)) and protons (Eq. (6)) by substituting in Eq. (5).

$$CH = \frac{^{t}C\,^{CH}K[H_p]}{1+^{CH}K[H_p]+\sqrt{^{CM1}K[M1_p]}+\sqrt{^{CM2}K[M2_p]}} \quad (7)$$

$$CM_{0.5} = \frac{^{t}C\sqrt{^{CM}K[M_p]}}{1+^{CH}K[H_p]+\sqrt{^{CM1}K[M1_p]}+\sqrt{^{M2}K[M2_p]}} \quad (8)$$

This isotherm is a specific case of the general multicomponent isotherm for any number of bound ions and several sites, that was described earlier for the biosorption of Cd, Cu, and Zn by protonated *S. fluitans* biomass in systems containing two metal ions and protons at different pH values [33]. *M* refers to either the first metal (*M*1) or the second one (*M*2).

In the next step, a combined Donnan-Biosorption-Isotherm equation was derived that allowed for direct calculation of cation binding without iterations. According to the Donnan theory, the equation for the concentration factor λ in an electrolytic gel is [34]

$$\lambda = \frac{[X_p]^{1/Z_x}}{[X]^{1/Z_x}} = \frac{[H_p]}{[H]} = \frac{[Na_p]}{[Na]} = \sqrt{\frac{[M_p]}{[M]}}\frac{[L]}{[M_p]} \quad (9)$$

$[X_p]$ is the concentration of any ionic species *X* with the charge Z_x in the gel.

The amount of coordinately bound metal (Eq. (8)) is substituted into Eq. (2), replaced $[X_p]$ in terms of [*X*] and λ (Eq. (9)) after dividing denominator and numerator of the left-hand term by λ, and the following relationship is obtained [34]:

$$^{M}q = \frac{^{t}C\sqrt{^{CM}K[M]}}{\frac{1}{\lambda}+^{CH}K[H]+\sqrt{^{CM1}K[M1]}+\sqrt{^{CM2}K[M2]}} + 2[M](\lambda^2-1)V_m \quad (10)$$

For the specific case that swelling of *Sargassum* particles linearly increases with the number of free sites ($V_m = Y_v C$, Y_v is a constant), the isotherm can be further simplified so that ^{M}q can be calculated directly without iterations.

$$^{M}q = \frac{^{t}C(\sqrt{^{CM}K[M]}+2[M]Y_V(\lambda-1/\lambda))}{\frac{1}{\lambda}+^{CH}K[H]+\sqrt{^{CM1}K[M1]}+\sqrt{^{CM2}K[M2]}} \quad (11)$$

An equation for proton binding can also be derived as

$$^{H}q = \frac{^{t}C(^{CH}K[H]+[H]Y_V(1-1/\lambda))}{\frac{1}{\lambda}+^{CH}K[H]+\sqrt{^{CM1}K[M1]}+\sqrt{^{CM2}K[M2]}} \quad (12)$$

By using the Eqs. (11) and (12), it is possible to calculate the binding of two-metal ions and protons without iteration. Schiewer and Volesky using the parameters, amount of binding sites, proton binding constant, and specific particle volume predicted the effect of pH, ionic strength, and Ca concentration on Cd binding of the *Sargassum* biomass [34].

MATHEMATICAL MODELLING OF DYNAMIC BIOSORPTION IN PACKED BED COLUMNS

Dynamic sorption studies are invariably more demanding. The most optimal configuration for continuous flow biosorption is the packed bed column which gets gradually saturated from the feed to the solution exit end.

The Adams-Bohart and Wolborska Models

Much work has been performed about the prediction of breakthrough curves in the sorption of the solute by the sorbents. Bohart and Adams proposed a model considering the breakthrough curve as symmetrical. This model is used for the description of the initial part of the breakthrough curve [36]. The mass transfer rates obey the following equations:

$$\frac{\partial q}{\partial t} = -kqC \tag{13}$$

$$\frac{\partial C}{\partial Z} = -\frac{k}{U_o} qC \tag{14}$$

where q is the metal ion content in the sorbent at t, C the solute concentration in solution, Z the column depth, k the kinetic constant and U_o the linear flow rate. Some assumptions are made for the solution of the differential equation system: (i) the concentration field is considered to be low, *e.g.* effluent concentration $C_s < 0.15C_o$; (ii) for $t \rightarrow \infty$, $q\ \rho \rightarrow N_o$, ρ is the apparent volumic mass of the sorbent in the packed bed and N_o the saturation concentration. The following equation is obtained, with parameters k and N_o [37]:

$$\ln\frac{C_s}{C_o} = kC_o t - kN_o\frac{Z}{U_o} \tag{15}$$

Wolborska shows that the mass transfer in the fixed-bed sorption obeys the following equations [38]:

$$\frac{\partial C}{\partial t} + U_o\left(\frac{\partial C}{\partial Z}\right) + \left(\frac{\partial q}{\partial t}\right) = D\left(\frac{\partial^2 C}{\partial Z^2}\right) \tag{16}$$

$$\frac{\partial q}{\partial t} = -v\left(\frac{\partial q}{\partial z}\right) = \beta_a(C - C_i) \tag{17}$$

where q is the solute concentration in the solid phase, C_i the solute concentration at the solid/liquid interface, D the axial diffusion coefficient, v the migration rate and β_a the kinetic coefficient of the external mass transfer. Making some assumptions such as $C_i << C$, $v << U_o$ and axial diffusion negligible $D \rightarrow 0$ as $t \rightarrow 0$, the solution can be approximated to:

$$\ln\frac{C_s}{C_o} = \frac{\beta_a C_o}{N_o} t - \frac{\beta_a Z}{U_o} \tag{18}$$

with

$$\beta_a = \frac{U_o^2}{2D}\left(\sqrt{1 + \frac{4\beta_o D}{U_o^2}} - 1\right) \tag{19}$$

where β_o is the external mass transfer coefficient with a negligible axial dispersion coefficient D. β_a is an effective coefficient which reflects the effect of both mass transfer in the liquid phase and axial diffusion. Wolborska observed that in short beds or at high flow rates of solution through the bed, the axial diffusion is negligible and $\beta_a = \beta_o$, the external mass transfer coefficient [38]. Assuming that the process conditions are steady for low concentrations of the breakthrough curve and the sorption isotherm is convex, the migration velocity of the steady-state front satisfies the relation, known as Wicke's law:

$$v = \frac{U_o C_o}{N_o + C_o} \tag{20}$$

The expression of the Wolborska solution is equivalent to the Adams-Bohart relation if the coefficient k is equal to β_a/N_o. So the drawing of $\ln C_s/C_o$ versus t would give information on both models [37].

Guibal *et al.* investigated static and dynamic removal of uranyl ions by silica gel and they reported that column studies showed a good correlation between the experimental data and the calculated breakthrough curves obtained by the Adams-Bohart or related derived models, and the Clark model [37]. Adams-Bohart, and related models, allow some mass transfer coefficients to be estimated, particularly the kinetic constant k. This coefficient varies between 1.2×10^{-4} and 2.5×10^{-3} L mg^{-1} min^{-1} for the uranium sorption by silica gel. The migration velocity v was calculated by the Wolborska method and the values are set between 3.9 and 22 $\times 10^{-3}$ m/h and the mass transfer coefficient β_a between 10 and 80 min^{-1} [37]. Amino-nitrogen of chitin and chitosan, important fungal cell wall components, is the main component responsible for heavy metal biosorption. The dynamic removal of hexavalent chromium by chitin flakes was studied in a packed column reactor [39]. The values of column parameters were predicted as a function of flow rate, bed depth, particle size and inlet metal ion concentration. The simulated breakthrough curves at an inlet Cr(VI) ion concentration of 50 mg/L and in a particle size ranges 595-420 and 841-595 μm for 6 cm bed depth are given in Fig. 1. This figure shows the superposition of experimental results (points) and theoretical calculated points (lines). It appears that the breakthrough is well predicted by Adams-Bohart, or derived models, whereas the whole breakthrough curve can not be defined. Effect of initial Cr(VI) ion concentration on the breakthrough curve of Cr(VI) sorption by chitin with the Adams-Bohart model in a particle size range 841-595 μm for 6.0 cm bed depth is also given in Fig. 2. The kinetic constant k varies between 0.83×10^{-4}

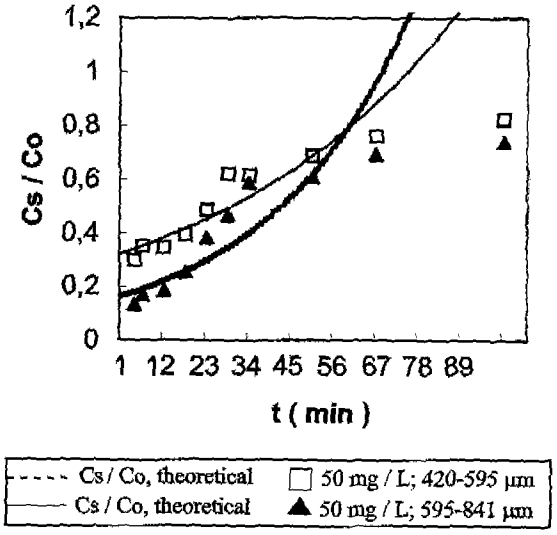

Fig. 1. Effect of particle size on the breakthrough curve of Cr(VI) sorption by chitin with the Adams-Bohart model. Lines are calculated curves, points are experimental data (Flow rate, 2.5 mL/min; bed depth, 6.0 cm).

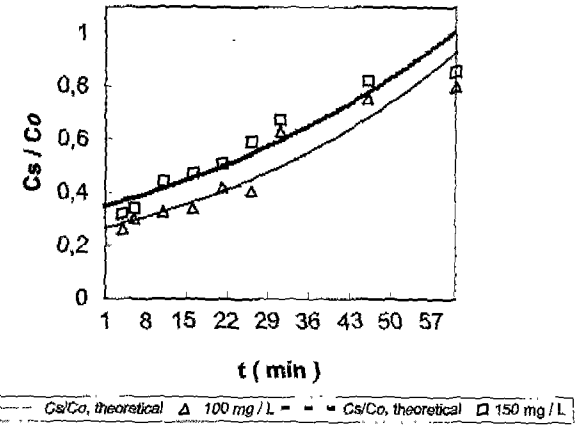

Fig. 2. Effect of initial metal ion concentration on the breakthrough curve of Cr(VI) sorption by chitin with the Adams-Bohart model. Lines are calculated curves, points are experimental data (Flow rate, 2.5 mL/min; bed depth, 6.0 cm; particle size, 841-595 μm).

and 6.17×10^{-4} L mg^{-1} min^{-1} [39]. These results are consistent with previous study on uranium sorption onto silica gel [37]. The migration velocity v changes between 2.55×10^{-2} and 18.36×10^{-2} m/h and the mass transfer coefficient β_a between 11.54 and 48.02 h^{-1} [39].

Clark Model

Clark's modelling associates the Freundlich equation and the mass transfer concept according to Eq. (21):

$$U_o \frac{dC}{dZ} = k_T (C - C_{eq}) \tag{21}$$

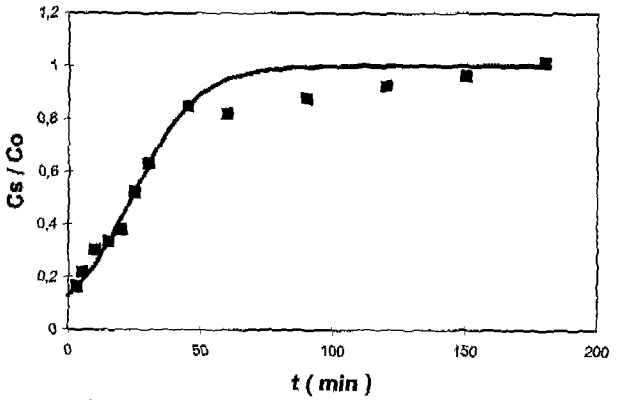

Fig. 3. The breakthrough curve of Cr(VI) sorption by chitin with the Clark model. Lines are calculated curves, points are experimental data (Initial metal ion concentration, 150 mg/L; flow rate, 2.5 mL/min; bed depth, 6.0 cm; particle size, 595-420 μm).

where k_T is the mass transfer rate coefficient. Clark resolved this system and obtained the following solution [40]:

$$\left(\frac{C_o^{n-1}}{1 + \left[\left(\frac{C_o^{n-1}}{C_b^{n-1}} - 1 \right) e^{rt_b} \right] e^{-rt}} \right)^{1/n-1} = C_s \tag{22}$$

where $R(n-1) = r$, $\quad R = \frac{k_T}{U_o} v$ (23)

Eq. (22) is the generalized logistic function. v, n, C_b and t_b are the migration velocity, the Freundlich constant, the concentration at breakthrough, and the time at breakthrough, respectively. For the Cr(VI) sorption onto chitin, a simulated breakthrough curve at an inlet Cr(VI) ion concentration of 150 mg/L and in a particle size range 420-595 μm for 6 cm bed depth is given in Fig. 3. For this breakthrough curve, the best fit equation is

$$C_s = \left(\frac{C_o^{1.02}}{1 + 6.76 e^{-0.0804t}} \right)^{0.977} \tag{24}$$

The effect of particle size on the breakthrough curve of Cr(VI) sorption by chitin with the Clark model for 6.0 cm bed depth is given in Fig. 4. It appears that the simulation of the whole breakthrough curve is effective with the Clark model, whereas the Adams-Bohart model gives good approximations of experimental behavior for the beginning of the piercing. At an initial metal ion concentration equal to 250 mg/L, varying particle size seems to have a reduced effect. Guibal *et al.* reported r coefficients changing between 1.18×10^{-2} and 14.94×10^{-2} min^{-1} with experimental parameters for uranium sorption by silica gel at similar column heights and flow rates [37]. The same order of magnitude for the r coefficient was obtained for Cr(VI) sorption by chitin. The r coefficient related to the mass transfer

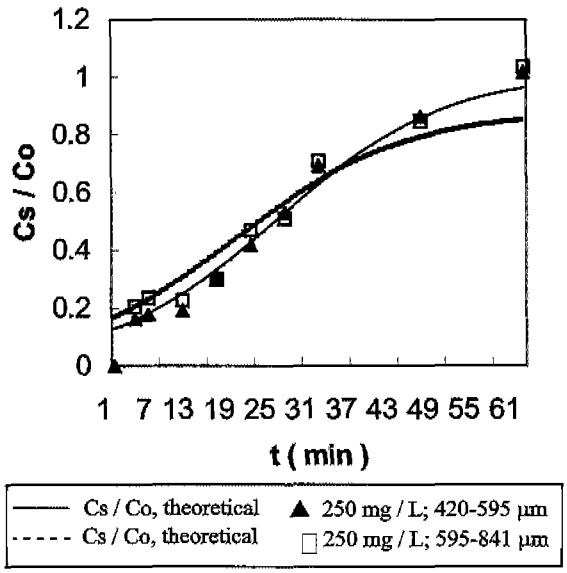

Fig. 4. Effect of particle size on the breakthrough curve of Cr(VI) sorption by chitin with the Clark model. Lines are calculated curves, points are experimental data (Flow rate, 2.5 mL/min; bed depth, 6.0 cm).

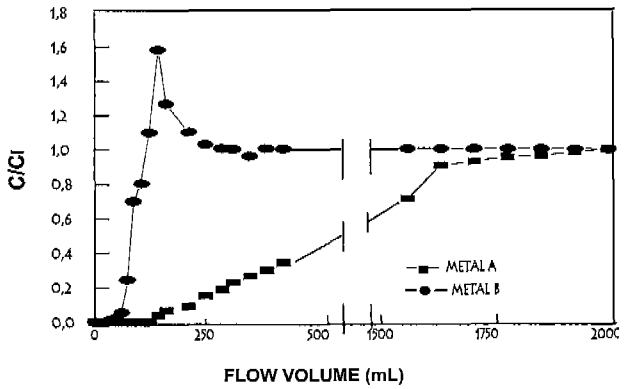

Fig. 5. The breakthrough curves for the simultaneous biosorption of two-metal ions at an equal inlet metal ion concentration. The overshoot depends on the relative affinities of the individual metals for the biosorbent. As Metal B overshoot occurs before Metal A breakthrough, column operation may have to be terminated at the overshoot time of Metal B [15].

varies between 0.38×10^{-2} and 62.1×10^{-2} min^{-1} [39].

The performance of packed-bed column is related to the length and shape of the ion-exchange zone. This zone develops between the section of the column that is saturated with heavy metal and the section that still contains fresh biosorbent. As the loading of the biosorbent progresses, the zone moves along the column. When the biosorbent saturation zone approaches the end of the column, the metal concentration in the outlet stream increases sharply and the effective life of the column is over [30]. One of the difficulties in describing the biosorption of heavy metal ions from waste streams is that waste waters contain not one but many metal ions. When several components are present, interference and competititon phenomena for sorption sites occur and lead to a more complex mathematical formulation of the equilibrium. The complex overlapping breakthrough curves for multicomponent mixtures where dispersive and non equilibrium effects are important cannot be described easily [15]. Biosorption in columns involves competitive ion exchange, in which several toxic heavy metals compete for a limited number of binding sites. When the column capacity is approached, a species with a lower affinity is pushed off by other species with higher affinity and displacement of the species occurs. Owing to the competitive ion exchange taking place in the column, one or more of the metals present even at trace levels may overshoot the permissible limit in the column effluent well before the breakthrough point of the targeted metal, thereby considerably reducing the service time of the column [41]. However, occurrence of output-concentration overshoots and impact on heavy-metal removal have not been well investigated.

In all the breakthrough curves the normalized concentration, defined as the measured concentration divided by the inlet concentration, is plotted against volumes of synthetic aqueous solutions treated. Breakthrough occurs when that metal appears in the effluent. When a binary metal mixture containing the metal ions at an equal concentration is pumped through the column of biomass, the representative breakthrough curves are given in Figs. 5 and 6. Metal B binds rapidly but not strongly (Fig. 5). Metal A binds slowly but binds almost irreversibly. Metal B binds first, then is pushed off by Metal A. When the biosorbent capacity is approached, Metal A with a higher affinity appears to displace Metal B with lower affinity. The sorption and displacement of metal ions is the reason for the outlet concentrations sometimes rising to values greater than 1. The metal B concentration reaches a maximum value in the effluent when Metal A breaks through. This type of overshoot shortens the processing time of the column [15]. In Fig. 6, a moderate amount of Metal B desorption even in the presence of excess Metal A concentration in the binary mixture is observed. This behaviour can imply that both metal ions bind strongly and/or there are a variety of binding sites on the biomass that are partially specific for individual metal species. The biosorption overshoot of Metal B does not interfere with the effective processing time of the column, because the overshoot time of Metal B is higher that the breakthrough time of the targetted Metal A. An unfavourable breakthrough curve is flat and trailing, indicating a wasteful long transfer zone inside the column. A favourable breakthrough curve is steep and sharp, showing the effective utilization of the biosorbent. The breakthrough curve obtained for the Metal B is completely unfavourable. On the other hand, the initial part of the breakthrough curve obtained for the Metal A is favourable, and the remain part is unfavour-

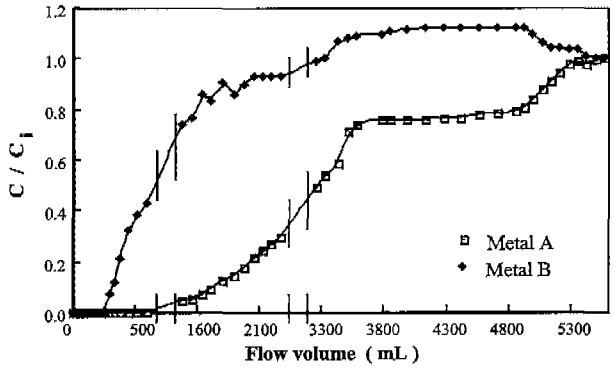

Fig. 6. The breakthrough curves for the simultaneous biosorption of two-metal ions at an equal inlet metal ion concentration. As Metal B overshoot occurs after Metal A breakthrough, the column can be operated right through to the breakthrough time of the Metal A [42].

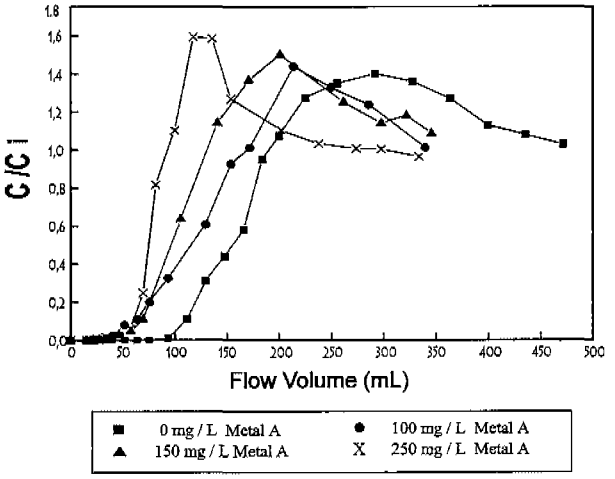

Fig. 7. The breakthrough curves of Metal B obtained at a constant inlet Metal B ion concentration of 250 mg/L but with increasing Metal A ion concentrations in the 0-250 mg/L range [15].

able because of dispersive and non equilibrium effects [42]. In Fig. 7, a series of breakthrough curves of Metal B ions obtained at a constant inlet concentrations of Metal B, but with increasing concentrations of Metal A is given. There appeared to be a significant inhibition in the uptake of Metal B in the presence of increasing concentrations of Metal A. Previously bound Metal B ions are eluted from the column by Metal A ions, giving a negative accumulation for the period when the metals are present in excess [15].

RECENT ADVANCES IN THE BIOSORPTION OF HEAVY METALS

The silica-immobilised cationic polyelectrolyte, [poly (*N*-xylene-*N*,*N*'-dicyclohexylethylenediamine dibromide)], capable of electrostatic binding with the biofilm of a natural alga *Spirogyras* sp., has been used in column separation for enrichment of trace analyte for detection by differential pulse anodic stripping voltammetry. Algae-silica preparation termed as AlgaSORB-sp involves the molecular-level polymer coating as 'spacer' between algae and silica gel. This system has been reported to be well suited for the continuous monitoring of heavy metals individually in aqueous medium and for the selective sorption of Cu(II) from multi-elemental systems [43].

Scant information is still available about the accumulation of metals in their complexed forms, as they are usually present in cyanide-containing industrial waste waters. There are, of course, reports on the treatment of metal cyanides using microorganisms. However, these studies mainly focus on biodegradation of metal cyanides. Recently, *Cladosporium cladosporioides* biomass has been shown to be a highly efficient biosorbent of copper cyanide and nickel cyanide from aqueous solutions [44]. Another study has attempted to elucidate the nature of metal-cell interaction of an *Aspergillus niger* during metal uptake from an industrial cyanide-containing solution. Au, Ag, Cu, Fe, and Zn were accumulated by *Aspergillus niger*, grown in an industrial gold mining solution containing cyano-metal complexes [45].

For the measurement of the metal biosorption potential of *Lemna*, *Microcystis* field-grown, *Microcystis* lab-grown, and *Spirogyra* from aqueous solution containing Pb, Cu, Cd and Zn in single, bi-, tri- and multimetallic mixture has been used differential pulse anodic stripping voltammetry (DPASV). Gravimetry, colorimetry, atomic absorption spectrophotometry (AAS), polarography are generally employed for measuring the metal concentration from solution. DPASV measurement technique, however, offers special advantage due to its high sensitivity and ease of application. In sharp contrast to AAS, the main advantage of DPASV is that simultaneous measurement of the concentration of several metals as well as their species from the same mixture can be achieved [46].

Up to now, the research on biosorption of heavy metals has mainly focused on either the adsorption efficiencies and equilibria for different biosorbent materials or the development of batch or continuous biosorption processes. However, relatively less work has been contributed to elucidate the details of the biosorption behavior in multi-metal systems, which are normally the composition of the industrial effluents. Two-metal biosorption studies are particularly important for assessing the degree of interference with a biosorption process of common metal ions in waste waters [47-49]. Often the prediction of sorption equilibria becomes more complicated by the presence of several sorbed ions, requiring the use of multi-component isotherm equations. Graphically, two-metal biosorption equilibria can be represented by adding another concentration axis to the conventional biosorption-isotherm plot, and then the isotherm curve will become a three-dimensional biosorption-isotherm surface [50,51]. To constract a 3-D

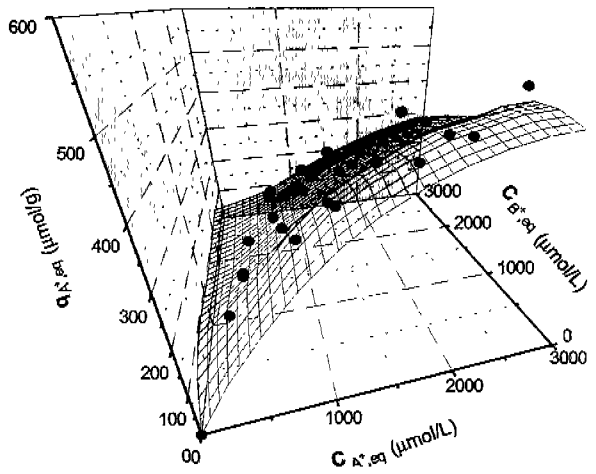

Fig. 8. A three-dimensional biosorption surface for the A+B biosorption system: q_{eq} (A^+) as a function of $C_{eq}(A^+)$ and $C_{eq}(B^+)$. The effect of B^+ presence on the A^+ uptake.

sorption isotherm plot, the metal uptake is plotted as a function of the final equilibrium concentrations of the two metals (Fig. 8). The computer program MATLAB 4.0 is capable of plotting a 3-D diagram based on randomly generated experimental data, fitting a smooth surface to the data according to the appropriate input equation, which represents the surface. The input equation is a multi-component sorption equilibrium model and a binary Langmuir-type equation was generally used in the literature [20,48]. In order to create the biosorption isotherm surfaces, an empirical extension of the Freundlich model, restricted to binary mixtures, was also used for the simultaneous biosorption of Cu(II) and Ni(II) ions by *Rhizopus arrhizus* [16].

Although this method can be extended to represent three-metal sorption equilibria (by a series of three dimensional 3-D plots whereby the residual concentration of one of the metals is taken as a parameter), a ternary system is represented in a triangular equilibrium diagram whereby the effect of the third ion is not ignored [20]. To use the triangular diagram, the final residual concentrations in solution, $C_{i,eq}$, and the metal uptakes, $q_{i,eq}$, are converted to metal mole fractions in solution, X_i, and mole fractions in the biosorbent, Y_i, respectively. In the triangular diagram, the equidistant axes refer to the mole fractions of the respective metal species on the biosorbent. Contour lines or parametric lines are superimposed on these axes (Fig. 9). It is possible to see the diagrams also as pseudo-4D plots (the result of projecting/viewing a series of the surfaces over the Gibbs triangle [52,53] from above). Triangular equilibrium diagrams were developed for the biosorption of Cu(II), Cd(II) and Zn(II) by *Ascophyllum nodosum* seaweed biomass [20], Cr(VI), Cu(II), and Fe(III) by *R. arrhizus* [54], and Cr(VI), Cu(II), and Cd(II) by *R. arrhizus* [55]. The former study used multicomponent Langmuir model, the latter two studies used both the multicomponent Langmuir and Freundlich models.

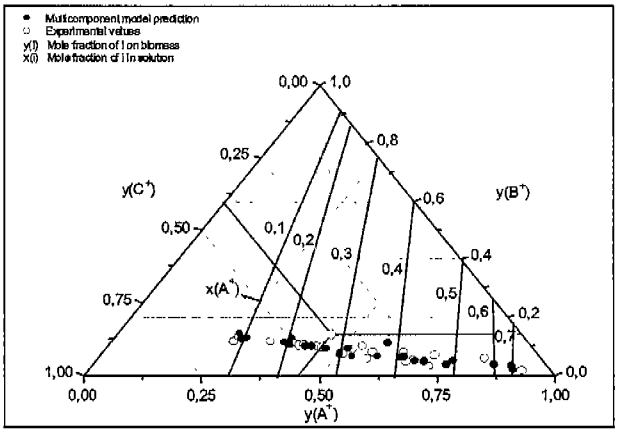

Fig. 9. A triangular equilibrium diagram. (—) Sorption isotherms of the constant A^+ fraction (solution).

Finally, as activated sludge is an attractive biosorbent because of its low cost and availability, combined effects of Ni(II) and Cr(VI) on living activated sludge [56], the biosorption of Zn(II) and Cu(II) on non-viable activated sludge from single and two-metal systems in a microcolumn adsorber configuration [57] and the effects of heavy metals, at sub-lethal concentrations, on activated sludge microbial ecosystem [58] have received great attention from researchers recently.

NOMENCLATURE

C	binding site or solute concentration in solution (mmol/L)
C_b	solute concentration at breakthrough (mmol/L)
C_{eq}	final equilibrium concentration of the residual sorbate remaining in the solution (mmol/L)
C_i	solute concentration at the solute/liquid interface (mmol/L)
C_o	column inlet concentration (mmol/L)
C_s	column effluent concentration (mmol/L)
D	axial diffusion coefficient (m^2/h)
H	protons
k	kinetic constant in the Adams-Bohart model (L mg^{-1} min^{-1})
k_T	mass transfer rate coefficient (min^{-1})
${}^{cm}K$	metal binding constant
${}^{CH}K_{app}$	apparent C site proton binding constant
M	divalent metal ions
n	Freundlich constant (dimensionless)
N_o	saturation concentration (mmol/L)
q	solute concentration in the solid phase or metal ion content in the sorbent at t (mmol/g)
q_{eq}	adsorbed sorbate quantity per unit weight of adsorbent at equilibrium (mmol/g)
r	coefficient related to the mass transfer in the Clark model (min^{-1})

t time (min)
t_b time at breakthrough (min)
U_o linear flow rate (m/h)
v migration velocity (m/h)
V_m specific volume (L/kg)
X any ionic species
$[X]$ concentrations of ionic species in the bulk solutions (mmol/L)
$[X_p]$ average concentration of X in the particle (mmol/g)
Z column depth (m)
Z_x charge

Greek Letters

λ concentration factor in an electrolytic gel (dimensionless)
ρ apparent volumic mass of the sorbent in the packed bed (g/L)
β_a effective coefficient which reflects the effect of both mass transfer in the liquid phase and axial diffusion in the Wolborska model (h^{-1})
β_o external mass transfer coefficient with a negligible axial dispersion coefficient in the Wolborska model (h^{-1})

REFERENCES

[1] Veglio, F. and F. Beolchini (1997) Removal of metals by biosorption: A review. *Hydrometallurgy* 44: 301-316.
[2] Tsezos, M. and B. Volesky (1982) The mechanism of uranium biosorption by *Rhizopus arrhizus*. *Biotechnol. Bioeng.* 24: 385-401.
[3] Kuyucak, N. and B. Volesky (1988) Biosorbents for recovery of metals from industrial solutions. *Biotechnol. Lett.* 10: 137-142.
[4] Tsezos, M. and B. Volesky (1981) Biosorption of uranium and thorium. *Biotechnol. Bioeng.* 23: 583-604.
[5] Remacle, J. (1990) The cell wall and metal binding. pp. 83-92. In: B. Volesky (ed.). *Biosorption of Heavy Metals*. CRC Press, Boca Raton, Florida, USA.
[6] Scott, J. A. and S. J. Palmer (1990) Sites of cadmium uptake in bacteria used for biosorption. *Appl. Microbiol. Biotechnol.* 33: 221-225.
[7] Brierley, C. L. (1990) Bioremediation of metal-contaminated surfaces and groundwaters. *Geomicrobiol. J.* 8: 201-223.
[8] Mann, H. (1990) Biosorption of heavy metals by bacterial biomass. pp. 93-138. In: B. Volesky (ed). *Biosorption of Heavy Metals*. CRC Press, Boca Raton, Florida, USA.
[9] Norberg, A. and H. Persson (1984) Accumulation of heavy metal ions by *Zoogloea ramigera*. *Biotechnol. Bioeng.* 26: 239-245.
[10] Chang, J. S. and J. Hong (1994) Biosorption of mercury by the inactivated cells of *Pseudomonas aeruinosa*. *Biotechnol. Bioeng.* 44: 999-1006.
[11] Bailey, J. E. and D. F. Ollis (1977) *Biochemical Engineering Fundamentals*. p. 15-21, 249. McGraw-Hill, NY, USA.
[12] Shuler, M. L. and F. Kargi, (1992) *Bioprocess Engineering: Basic Concepts*. Prentice Hall, Englewood Cliffs, New Jersey, USA.
[13] Volesky, B. (1990) Biosorption by fungal biomass. pp. 139-171. In: B. Volesky (ed). *Biosorption of Heavy Metals*. CRC Press, Boca Raton, Florida, USA.
[14] Huang, C. and C. P. Huang (1996) Application of *Aspergillus oryzae* and *Rhizopus oryzae* for Cu(II) removal. *Wat. Res.* 30: 1985-1990.
[15] Sağ, Y., I. Ataçoğlu, and T. Kutsal (1999) Simultaneous biosorption of chromium(VI) and copper(II) on *Rhizopus arrhizus* in packed column reactor: application of the competitive Freundlich model. *Sep. Sci. Technol.* 34: 3155-3171.
[16] Sağ, Y. (2001) Biosorption of heavy metals by fungal biomass and modeling of fungal biosorption: A review. *Separ. Purif. Method.* 30: 1-48.
[17] Sağlam, N., R. Say, A. Denizli, S. Patır, and M. Y. Arıca (1999) Biosorption of inorganic mercury and alkylmercury species on to *Phanerochaete chrysosporium* mycelium. *Process Biochem.* 34: 725-730.
[18] Muraleedharan, T.R. and C. Venkobachar (1990) Mechanism of biosorption of copper(II) by *Ganoderma lucidum*. *Biotechnol. Bioeng.* 35: 320-325.
[19] Rao, C. R. N., L. Iyengar, and C. Venkobachar (1993) Sorption of copper(II) from aqueous phase by waste biomass. *J. Environ. Eng.* 119: 369-377.
[20] Chong, K. H. and B. Volesky (1996) Metal biosorption equilibria in a ternary system. *Biotechnol. Bioeng.* 49: 629-638.
[21] Wang, T. C., J. C. Weissman, G. Ramesh, R. Varadarajan, and J. R. Benemann (1998) Heavy metal binding and removal by *Phormidium*. *Bull. Environ. Contamin. Toxicol.* 60: 739-744.
[22] Özer, D. Z. Aksu, T. Kutsal, and A. Çağlar (1994) Adsorption isotherms of lead(II) and chromium(VI) on *Cladophora crispata*. *Environ. Technol.* 15: 439-448.
[23] Holan, Z. R., B. Volesky, and I. Prasetyo (1993) Biosorption of cadmium by biomass of marine algae. *Biotechnol. Bioeng.* 41: 819-825.
[24] Volesky, B. Advances in biosorption of metals: Selection of biomass types. *FEMS Microbiol. Rev.* 14: 291-302.
[25] Kuyucak, N. and B. Volesky (1990) Biosorption by algal biomass. pp. 173-198. In: B. Volesky (ed). *Biosorption of Heavy Metals*. CRC Press, Boca Raton, Florida, USA.
[26] Wilde, E. W. and J. R. Benemann (1993) Bioremoval of heavy metals by the use of microalgae. *Biotechnol. Adv.* 11: 781-812.
[27] Fourest, E. and B. Volesky (1996) Contribution of sulfonate groups and alginate to heavy metal biosorption by the dry biomass of *Sargassum fluitans*. *Environ. Sci. Technol.* 30: 277-282.
[28] Kratochvil, D., E. Fourest, and B. Volesky (1995) Biosorption of copper by *Sargassum fluitans* biomass in a fixed bed column. *Biotechnol. Lett.* 17: 777-782.
[29] Yu, Q., J. T. Matheickal, P. Yin, and K. Pairat (1999) Heavy metal uptake capacities of common marine macro algal biomass. *Water Res.* 33: 1534-1537.
[30] Kratochvil, D. and B. Volesky (1998) Advances in the biosorption of heavy metals. *Trends Biotechnol.* 16: 291-300.
[31] Sağ, Y. and T. Kutsal (1995) Biosorption of heavy metals

by *Zoogloea ramigera*: Use of adsorption isotherms and a comparison of biosorption characteristics. *Chem. Eng. J.* 60: 181-188.
[32] McKay, G., Y. S. Ho, and J. C. Y. Ng (1999) Biosorption of copper from waste waters: A review. *Separ. Purif. Method.* 28: 87-125.
[33] Schiewer, S. and B. Volesky (1996) Modeling multi-metal ion exchange in biosorption. *Environ. Sci. Technol.* 30: 2921-2927.
[34] Schiewer, S. and B. Volesky (1997) Ionic strength and electrostatic effects in biosorption of divalent metal ions and protons. *Environ. Sci. Technol.* 31: 2478-2485.
[35] Schiewer, S. and B. Volesky (1997) Ionic strength and electrostatic effects in biosorption of protons. *Environ. Sci. Technol.* 31: 1863-1871.
[36] Bohart, G. and E. Q. Adams (1920) Some aspects of the behaviour of charcoal with respect to chlorine. *J. Am. Chem. Soc.* 42: 523-544.
[37] Guibal, E., R. Lorenzelli, T. Vincent, and P. Le Cloirec (1995) Application of silica gel to metal ion sorption: static and dynamic removal of uranyl ions. *Environ. Technol.* 16: 101-114.
[38] Wolborska, A. (1989) Adsorption on activated carbon of *p*-nitrophenol from aqueous solution. *Wat. Res.* 23: 85-91.
[39] Sağ, Y. and Y. Aktay (2001) Application of equilibrium and mass transfer models to dynamic removal of Cr(VI) ions by chitin in packed column reactor. *Process Biochem.* 36: 1187-1197.
[40] Clark, R. M. (1987) Evaluating the cost and performance of field-scale granular activated carbon systems. *Environ. Sci. Technol.* 21: 573-580.
[41] Trujillo, E. M., T. H. Jeffers, C. Freguson, and H. Q. Stevenson (1991) Mathematically modeling the removal of heavy metals from a waste water using immobilized biomass. *Environ. Sci. Technol.* 25: 1559-1565.
[42] Sağ, Y., I. Ataçoğlu, and T. Kutsal (2000) Equilibrium parameters for the single- and multicomponent biosorption of Cr(VI) and Fe(III) ions on *R. arrhizus* in a packed column. *Hydrometallurgy* 55: 165-179.
[43] Singh, R. and B. B. Prasad (2000) Trace metal analysis: selective sample (copper II) enrichment on an AlgaSORB column. *Process Biochem.* 35: 897-905.
[44] Patil, Y. B. and K. M. Paknikar (1999) Removal and recovery of metal cyanides using a combination of biosorption and biodegradation processes. *Biotechnol. Lett.* 21: 913-919.
[45] Gomes, N. C. M., M. M. Figueira, E. R. S. Camargos, L. C. S. Mendonça-Hagler, J. C. T. Dias, and V. R. Linardi (1999) Cyano-metal complexes uptake by *Aspergillus niger*. *Biotechnol. Lett.* 21: 487-490.
[46] Singh, S., S. Pradhan, and L. C. Rai (2000) Metal removal from single and multimetallic systems by different biosorbent materials as evaluated by differential pulse anodic stripping voltammetry. *Process Biochem.* 36: 175-182.
[47] Chang, J.-S. and C-C. Chen (1998) Quantitative analysis and equilibrium models of selective adsorption in multimetal systems using a bacterial biosorbent. *Separ. Sci. Technol.* 33: 611-632.
[48] Figueira, M. M., B. Volesky, and V. S. T. Ciminelli (1997) Assessment of interference in biosorption of a heavy metal. *Biotechnol. Bioeng.* 54: 344-350.
[49] Sağ, Y. and T. Kutsal (1996) Fully competitive biosorption of chromium(VI) and iron(III) ions from binary metal mixtures by *R. arrhizus*: Use of the competitive Langmuir model. *Process Biochem.* 31: 573-585.
[50] Chong, K. H. and B. Volesky (1995) Description of two-metal biosorption equilibria by Langmuir-type models. *Biotechnol. Bioeng.* 47: 451-460.
[51] de Carvalho, R. P., K.-H. Chong, and B. Volesky (1995) Evaluation of the Cd, Cu and Zn biosorption in two-metal systems using algal biosorbent. *Biotechnol. Prog.* 11: 39-44.
[52] Soldatov, V. S. and V. A. Bichkova (1980) Ternary ion-exchange equilibria. *Sep. Sci. Technol.* 15: 89-110.
[53] Soldatov, V. S. and V. A. Bichkova (1985) Binary ion exchange selectivity coefficients in multiionic systems. *React. Polym.* 3: 199-206.
[54] Sağ, Y., B. Akçael, and T. Kutsal (2001) Evaluation, interpretation, and representation of three-metal biosorption equilibria using a fungal biosorbent. *Process Biochem.* 37: 35-50.
[55] Sağ, Y., B. Akçael, and T. Kutsal (2002) Ternary Biosorption Equilibria of Chromium(VI), Copper(II), and Cadmium(II) on *Rhizopus arrhizus*. *Separ. Sci. Technol.* in press.
[56] Dilek, F. B., C. F. Gökçay, and Ü. Yetis (1998) Combined effects of Ni(II) and Cr(VI) on activated sludge. *Wat. Res.* 32: 303-312.
[57] Utgikar, V., B.-Y. Chen, H. H. Tabak, D. F. Bishop, and R. Govind (2000) Treatment of acid mine drainage: I. Equilibrium biosorption of zinc and copper on non-viable activated sludge. *Int. Biodeter. Biodegr.* 46: 19-28.
[58] Chua, H., P. H. F. Yu, S. N. Sin, and M. W. L. Cheung (1999) Sub-lethal effects of heavy metals on activated sludge microorganisms. *Chemosphere* 39: 2681-2692.

[Received July 30, 2001; accepted November 20, 2001]